PLOS ONE

RESEARCH ARTICLE

# A new approach to keratoconus detection based on corneal morphogeometric analysis

**Francisco Cavas-Martínez[1]*, Laurent Bataille[1,2,3], Daniel G. Fernández-Pacheco[1], Francisco J. F. Cañavate[1], Jorge L. Alió[3,4,5]**

**1** Department of Graphical Expression, Technical University of Cartagena, Cartagena, Spain, **2** Research and Development Department, Vissum Corporation Alicante, Spain, **3** Keratoconus Unit, Vissum Corporation Alicante, Spain, **4** Division of Ophthalmology, Universidad Miguel Hernández, Alicante, Spain, **5** Department of Refractive Surgery, Vissum Corporation Alicante, Spain

* francisco.cavas@upct.es

Check for updates

OPEN ACCESS

**Citation:** Cavas-Martínez F, Bataille L, Fernández-Pacheco DG, Cañavate FJF, Alió JL (2017) A new approach to keratoconus detection based on corneal morphogeometric analysis. PLoS ONE 12 (9): e0184569. https://doi.org/10.1371/journal.pone.0184569

**Editor:** Michele Madigan, Save Sight Institute, AUSTRALIA

**Received:** June 5, 2017

**Accepted:** August 26, 2017

**Published:** September 8, 2017

**Copyright:** © 2017 Cavas-Martínez et al. This is an open access article distributed under the terms of the Creative Commons Attribution License, which permits unrestricted use, distribution, and reproduction in any medium, provided the original author and source are credited.

**Data Availability Statement:** Data are available from the VISSUM Corporation Institutional Data Access / Ethics Committee for researchers who meet the criteria for access to confidential data. Contact information for the Vissum Corporation Institutional data access / Ethics Committee: clinicaltrials@vissum.com.

**Funding:** This publication has been carried out in the framework of the Thematic Network for Co-Operative Research in Health (RETICS) reference number RD12/0034/0007 and RD16/0008/0012,

## Abstract

### Purpose

To characterize corneal structural changes in keratoconus using a new morphogeometric approach and to evaluate its potential diagnostic ability.

### Methods

Comparative study including 464 eyes of 464 patients (age, 16 and 72 years) divided into two groups: control group (143 healthy eyes) and keratoconus group (321 keratoconus eyes). Topographic information (Sirius, CSO, Italy) was processed with SolidWorks v2012 and a solid model representing the geometry of each cornea was generated. The following parameters were defined: anterior ($A_{ant}$) and posterior ($A_{post}$) corneal surface areas, area of the cornea within the sagittal plane passing through the Z axis and the apex ($A_{apexant}$, $A_{apexpost}$) and minimum thickness points ($A_{mctant}$, $A_{mctpost}$) of the anterior and posterior corneal surfaces, and average distance from the Z axis to the apex ($D_{apexant}$, $D_{apexpost}$) and minimum thickness points ($D_{mctant}$, $D_{mctpost}$) of both corneal surfaces.

### Results

Significant differences among control and keratoconus group were found in $A_{apexant}$, $A_{apexpost}$, $A_{mctant}$, $A_{mctpost}$, $D_{apexant}$, $D_{apexpost}$ (all $p<0.001$), $A_{post}$ ($p = 0.014$), and $D_{mctpost}$ ($p = 0.035$). Significant correlations in keratoconus group were found between $A_{ant}$ and $A_{post}$ ($r = 0.836$), $A_{mctant}$ and $A_{mctpost}$ ($r = 0.983$), and $D_{mctant}$ and $D_{mctpost}$ ($r = 0.954$, all $p<0.001$). A logistic regression analysis revealed that the detection of keratoconus grade I (Amsler Krumeich) was related to $A_{post}$, $A_{tot}$, $A_{apexant}$, $A_{mctant}$, $A_{mctpost}$, $D_{apexpost}$, $D_{mctant}$ and $D_{mctpost}$ (Hosmer-Lemeshow: $p>0.05$, $R^2$ Nagelkerke: 0.926). The overall percentage of cases correctly classified by the model was 97.30%.

### Conclusions

Our morphogeometric approach based on the analysis of the cornea as a solid is useful for the characterization and detection of keratoconus.

financed by the Carlos III Health Institute – General Subdirection of Networks and Cooperative Investigation Centers (R&D&I National Plan 2008–2011) and the European Regional Development Fund (FEDER). The funders had no role in study design, data collection and analysis, decision to publish, or preparation of the manuscript.

**Competing interests:** The private ophthalmology clinic VISSUM and all the authors from this private clinic do not have any competing interests (financial, non-financial, professional, or personal) in this research submitted to the journal.

## Introduction

Keratoconus is an ectatic corneal disorder characterized by progressive corneal thinning and structural weakening and resulting in corneal protrusion, irregular astigmatism, and decreased vision [1]. Several diagnostic criteria have been defined using a great variety of techniques and technologies [2]. Besides classical keratoconus biomicroscopic signs [3], the conical protrusion and infero-superior asymmetry associated to keratoconus can be easily detected by means of corneal topography [3–5]. Problems arises when very incipient stages of keratoconus are intended to be detected (subclinical keratoconus). In such cases, a more comprehensive analysis of corneal geometry is necessary as well as the consideration of other complementary descriptors, such as corneal aberrations, pachymetry, asphericity, or the analysis of corneal biomechanical properties [6–14].

The correlation between the anterior and posterior corneal shape in keratoconus has been also investigated [14, 15] and its potential diagnostic value have been also even evaluated [4]. A comprehensive analysis of this relationship can be performed by means of geometric modeling enabling the characterization of the human cornea [16]. We previously validated the use of some new indices based on an innovative morphogeometric modeling of the corneal structure for the detection of keratoconus [16]. The current study is a continuation of this research by confirming the diagnostic ability of the morphogeometric indices developed but in a larger sample of patients as well as by creating a new predictive model of detection of incipient keratoconus based on the combination of such indices.

## Material and methods

### Patients

This was a comparative study including 464 eyes of 464 patients ranging in age between 16 and 72 years old. Only one eye from each patient was randomly selected for the study according to a random number sequence (dichotomic sequence, 0 and 1) that was created with specific software in order to avoid the interference in the analysis of the correlation that often exists between the two eyes of the same person. This study was conducted at Vissum Corporation in Alicante (Spain). Two groups of eyes were differentiated depending if the keratoconus disease was present or not: control group, including 143 healthy eyes, and keratoconus group, including 321 eyes with the diagnosis of keratoconus. The inclusion criterion for the control group was healthy eyes that did not meet the exclusion criteria and diagnosis according to the standard criteria for keratoconus diagnosis in the keratoconus group [2, 3], which is the presence of an asymmetric bowtie pattern in corneal topography, a value of 100 or higher of the KISA index, a central keratometry (K-value) with different cut-off values to keratoconus suspect (>47.2 D), a inferior-superior asymmetry (I-S value) with a cut-off value of 1.4 D difference between average inferior and superior corneal powers at 3 mm from the center of the cornea, as well as other topographic indices (SRAX, KSS, KPI, CLMI) and at least one keratoconus sign on slit-lamp examination, such as stromal thinning, conical protusion on the cornea at the apex, Fleischer ring, Vogt striae or anterior stromal scar. Exclusion criteria in both groups were previous ocular surgery and any other active ocular disease. Patients with forme fruste keratoconus (with topographic alterations compatible with keratoconus but without apparent clinical alterations of this pathology (normal visual acuity = 1.00)) and patients with normal eyes but with a keratoconic contralateral eye were not included in this study. The study was approved by the Vissum Corporation ethics committee and was then performed in accordance with the ethical standards laid down in the Declaration of Helsinki (Seventh revision, October 2013, Fortaleza, Brasil). A supplementary file (S1 Table) including the following

patients' data is provided: age, gender, contact lens wear, both eyes affected, studied eye, K2 and central thickness.

## Examination protocol

All patients underwent a complete eye examination including the following tests: anamnesis, measurement of uncorrected (UDVA) and corrected (CDVA) distance visual acuity, manifest refraction, slit-lamp biomicroscopy, and corneal analysis by the Sirius system (Costruzione Strumenti Oftalmici, Italy). Repeatability of the topographic measurements provided by the Sirius system in keratoconic eyes are demonstrated in previous studies [17]. All tests were performed by a single experienced examiner. A minimum of three corneal topographies were successively obtained for each cornea and the best one (the topography with the highest acquisition quality for the Scheimpflug image and keratoscopy) selected to provide data for this study. All corneal topography files were exported in.csv format. Likewise, all cases were classified according to the Amsler-Krumeich grading system [1].

## Geometric modeling

The morphogeometric modeling was performed following a procedure previously described and validated by our research group [16]. In general terms, this method consisted of the following steps:

- Preparation of the point cloud. A surface from the geometry that a point cloud presents was generated in a coordinate system for a three-dimensional space. Topography files exported in.csv were formatted in Cartesian coordinates by an algorithm programmed using Matlab software. For such purpose, it was considered that every row represents a circle in the corneal map and every column represents a semi-meridian, providing a total of 256 points for each radius. Each i-th row sampled a map on a circle of i*0.2 mm radius, and each j-th column sampled a map on a semimeridian in the direction of j*360/256u, so each Z value of the matrix [i, j] represented the point P (i*0.2, j*360/256u) in polar coordinates. The geometric center of the cornea was obtained from the XYZ coordinates provided by the topographer, which correspond to the center of the Placido disc rings. Specifically, the point cloud was generated for the area from the corneal geometric center (r = 0 mm) to the beginning of the so-called peripheral zone (r = 4 mm). It should be taken into account that this area of analysis is considered to have more information on corneal morphology for both healthy and diseased eyes [16].
- Geometric Surface Reconstruction. The point cloud representing the corneal geometry was imported into the surface reconstruction software Rhinoceros v5.0. The surface that best fits the point cloud was generated with the Rhinoceros's patch surface function that tries to minimize the nominal distance between the 3D point cloud and the solution surface. The settings of the function were configured as follows: sample point spacing 256, surface span planes 255 for both u and v directions, and stiffness of the solution surface.
- Solid Modeling. The resulting surface was imported into the solid modeling software SolidWorks v2012. With this software, the solid model representing the custom and actual geometry of each cornea was generated.
- Definition of the morphogeometric variables to analyze. From the solid model obtained, the following geometric variables were defined (Table 1):
    - Anterior corneal surface area ($mm^2$) ($A_{ant}$): area of the anterior corneal surface of the solid model generated (Fig 1)

**Table 1. List of acronyms used for the morphogeometric variables of the study.**

| Acronym | Description |
|---|---|
| $A_{ant}$ | Anterior corneal surface area |
| $A_{post}$ | Posterior corneal surface area |
| $A_{tot}$ | Total corneal surface area |
| $A_{apexant}$ | Sagittal plane area at anterior apex |
| $A_{apexpost}$ | Sagittal plane area at posterior apex |
| $A_{mctant}$ | Sagittal plane area at anterior minimum thickness point |
| $A_{mctpost}$ | Sagittal plane area at posterior minimum thickness point |
| $D_{apexant}$ | Anterior apex deviation |
| $D_{apexpost}$ | Posterior apex deviation |
| $D_{mctant}$ | Anterior minimum thickness point deviation |
| $D_{mctpost}$ | Posterior minimum thickness point deviation |

https://doi.org/10.1371/journal.pone.0184569.t001

- Posterior corneal surface area ($mm^2$) ($A_{post}$): area of the posterior corneal surface of the solid model generated (Fig 1)
- Total corneal surface area ($mm^2$) ($A_{tot}$): sum of anterior, posterior and perimetral corneal surface areas of the solid model generated
- Sagittal plane apex area ($mm^2$): area of the cornea within the sagittal plane passing through the Z axis and the highest point (apex) of the anterior ($A_{apexant}$) or posterior ($A_{apexpost}$) corneal surface (Fig 2)
- Sagittal plane area at minimum thickness point ($mm^2$): area of the cornea within the sagittal plane passing through the Z axis and the minimum thickness point of the anterior ($A_{mctant}$) and posterior ($A_{mctpost}$) corneal surfaces
- Anterior and posterior apex deviation (mm): average distance from the Z axis to the highest point (apex) of the anterior ($D_{apexant}$) and posterior corneal surfaces ($D_{apexpost}$) (Fig 3)
- Anterior and posterior minimum thickness point deviation (maximum curvature) (mm): average distance in the XY plane from the Z axis to the minimum thickness points (maximum curvature) of the anterior ($D_{mctant}$) and posterior corneal surfaces ($D_{mctpost}$) (Fig 4)

## Statistical analysis

SPSS statistics software package version 15.0 (IBM, Armonk, EEUU) was used for the statistical analysis. Normality of all data was checked by means of the Kolmogorov-Smirnov test. A comparison between healthy and keratoconus groups was performed with the unpaired Student t or Mann-Whitney U tests depending if the data samples were normally distributed or not. An additional analysis was performed to compare differences between groups according to keratoconus stages graded using the Amsler-Krumeich classification system. The one-way analysis of variance (ANOVA) was used for such purpose if variables were normally distributed, whereas the Kruskal-Wallis test was used if one or more variables were not normally distributed. The post-hoc comparative analysis for the ANOVA was performed with the Bonferroni test when the variances were homogeneous and the T2 Tamhane test when the variances were not homogeneous, while the Mann-Whitney tests with the Bonferroni´s adjustment was used for the post-hoc analysis of the Kruskal-Wallis test. Pearson and Spearman correlation coefficients were used to assess the correlation between anterior and posterior geometric parameters depending if the data samples were or not normally distributed. Differences were considered to be statistically significant when the associated p-value was $<0.05$.

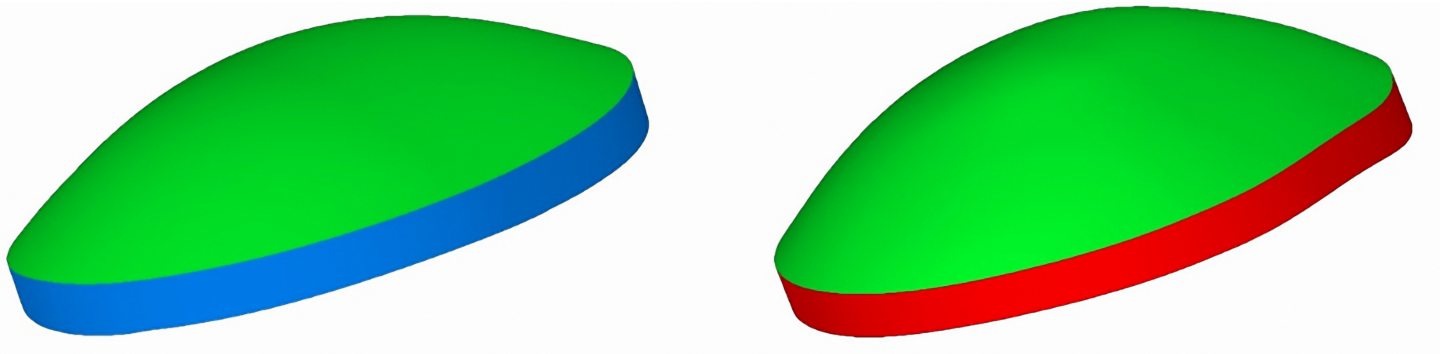

**Fig 1. Area of the anterior corneal surface in the solid model generated for a specific cornea evaluated in the current study (green) compared to a healthy (blue) and keratoconus cornea (red).**

https://doi.org/10.1371/journal.pone.0184569.g001

A stepwise backward logistic regression was also performed to define the key parameters involved in the detection of keratoconus grade I as moderate and severe keratoconus can be easily detected by means of topographic and biomicroscopic analysis. Hosmer-Lemeshow adjustment was used to assess the overall goodness of fit of the model, and $R^2$ Cox and Snell and $R^2$ Nagelkerke were used to study the variance rate explained by the variables of the model. The specific relationship between the parameters of the final model was evaluated with the model coefficients (B) and the odds ratios that represent the value of increased likelihood that a category of the dependent variable is met for each unit of the independent variable, while the other independent variables are held constant. Finally, the efficacy of the model to detect keratoconus grade I was compared with that provided by the classifier of the topography system used for obtaining the measurements. This classifier is based on the use of different indices obtained from both the anterior and posterior corneal surfaces, including symmetry index of front and back corneal curvature, best fit radius of the front corneal surface, Baiocchi Calossi Versaci front index (BCV(f)) and BCV back index (BCV(b)), root mean square of front and back corneal surface higher order aberrations, and thinnest corneal point [18].

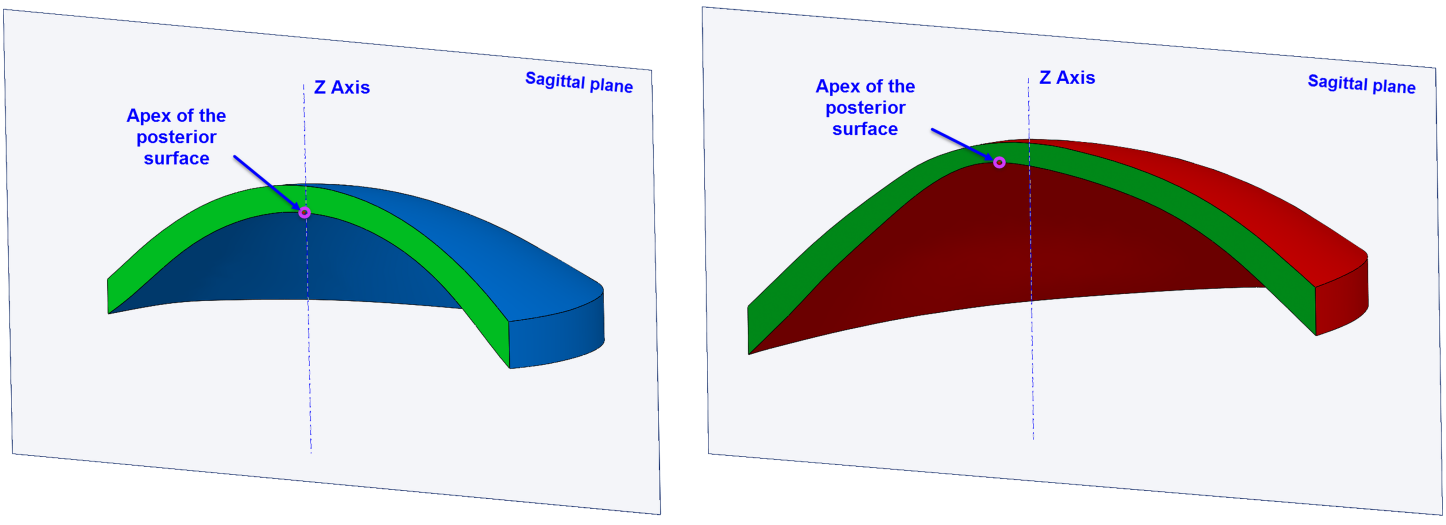


**Fig 2. Area of the cornea within the sagittal plane passing through the Z axis and the highest point (apex) of the posterior corneal surface in a healthy (blue) and keratoconus cornea (red).**

https://doi.org/10.1371/journal.pone.0184569.g002

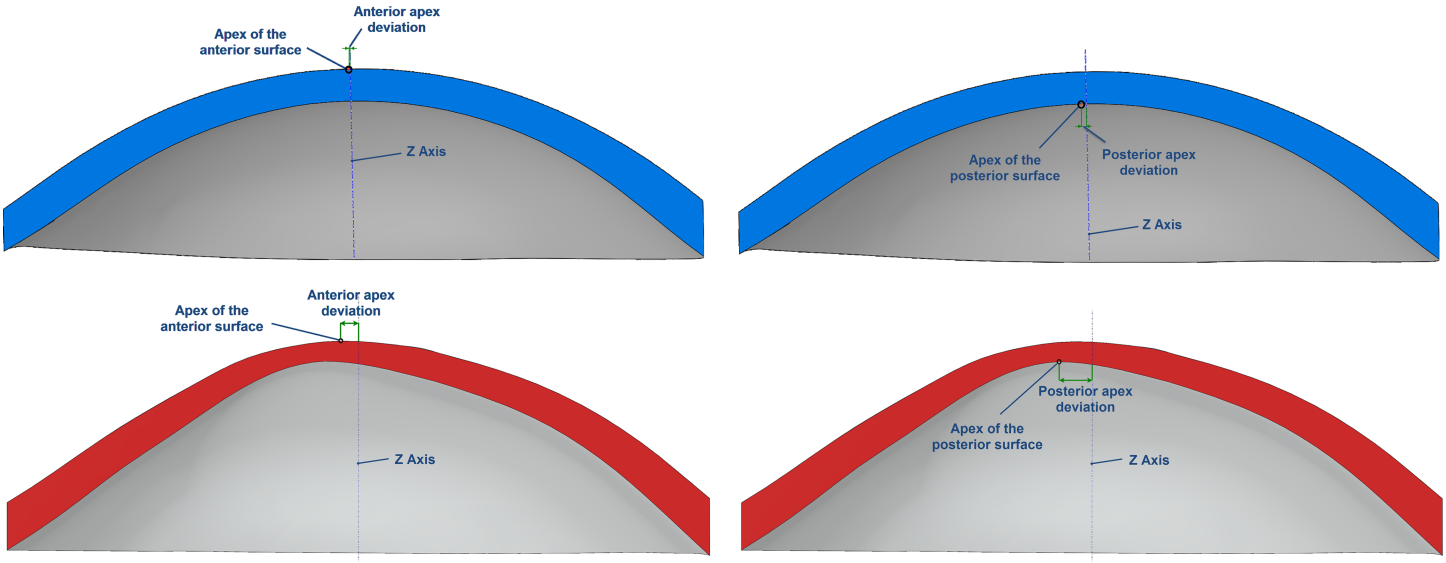


**Fig 3. Average distance from the Z axis to the highest point (apex) of the anterior and posterior corneal surfaces in a healthy (blue) and keratoconus cornea (red).**

https://doi.org/10.1371/journal.pone.0184569.g003

## Results

A total of 143 healthy eyes of 143 patients (30.8%) (control group) and 321 keratoconus eyes of 321 patients (69.2%) (keratoconus group) were enrolled in the study. In the keratoconus group, the following subgroups were differentiated according to the stage of the disease following the Amsler-Krumeich grading system: grade I (229 eyes, 71.3%), grade II (59 eyes, 18.4%), grade III (9 eyes, 2.8%), and grade IV (24 eyes, 7.5%).

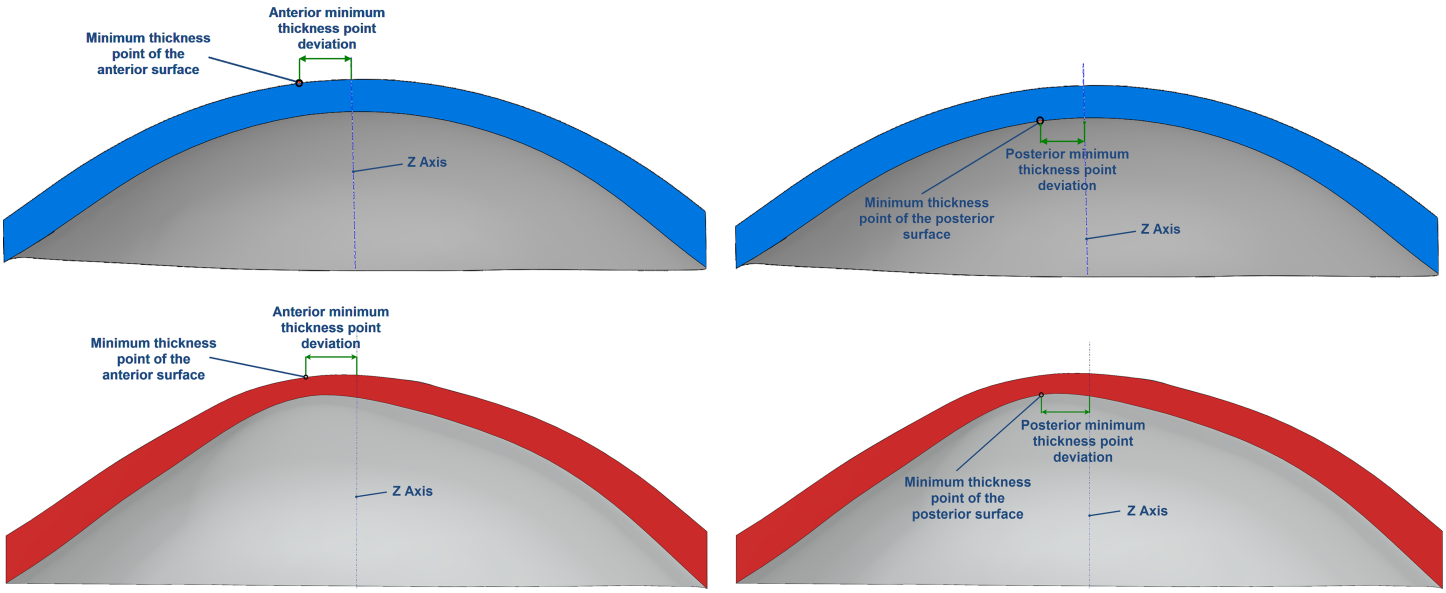


**Fig 4. Average distance in the XY plane from the Z axis to the minimum thickness points (maximum curvature) of the anterior and posterior corneal surfaces in a healthy (blue) and keratoconus cornea (red).**

https://doi.org/10.1371/journal.pone.0184569.g004

## Comparison control vs. keratoconus group

Table 2 summarizes the outcomes obtained in the control and keratoconus group. Significant differences among control and keratoconus group were found in $A_{post}$ ($p = 0.014$), $A_{apexant}$ ($p<0.001$), $A_{apexpost}$ ($p<0.001$), $A_{mctant}$ ($p<0.001$), $A_{mctpost}$ ($p<0.001$), $D_{apexant}$ ($p<0.001$), $D_{apexpost}$ ($p<0.001$), and $D_{mctpost}$ ($p = 0.035$). Specifically, in keratoconus group, significantly higher values of $A_{post}$, $A_{apexant}$, $D_{apexant}$, $D_{apexpost}$ and $D_{mctpost}$ as well as lower values of $A_{apexpost}$, $A_{mctant}$ and $A_{mctpost}$ compared to control group.

Table 3 summarizes the outcomes obtained in the control group and keratoconus subgroups according to the stage of severity of the disease. An extended version of the table is also provided as supplementary file (S2 Table). Significant differences among keratoconus stages were found in the geometric parameters evaluated ($p<0.001$). Specifically, significant differences were found among all keratoconus subgroups were found for $A_{post}$ ($p\leq0.001$). Significant differences were found between control group and keratoconus grade I subgroups for all parameters ($p\leq0.021$) except for $D_{mctant}$ ($p\geq0.056$).

## Correlation between anterior and posterior corneal geometry parameters

Table 4 summarizes the correlations obtained between the geometric parameters of the anterior and posterior corneal surfaces in the control group and keratoconus group as well as in

**Table 2. Summary of the outcomes obtained in control and keratoconus groups.**

| Mean (SD) Median (Range) | Control | Keratoconus | p-valor (test) |
|---|---|---|---|
| $A_{ant}$ ($mm^2$) | 43.08 (0.14)<br>43.08 (42.73 to 43.39) | 43.12 (0.56)<br>43.00 (42.00 to 47.00) | 0.435 |
| $A_{post}$ ($mm^2$) | 44.24 (0.28)<br>44.24 (43.49 to 44.90) | 44.43 (0.89)<br>44.00 (43.00 to 51.00) | 0.014 |
| $A_{tot}$ ($mm^2$) | 103.92 (1.20)<br>103.88 (100.69 to 106.15) | 103.64 (1.91)<br>103.00 (99.96 to 114.00) | 0.106 |
| $A_{apexant}$ ($mm^2$) | 0.24 (1.01)<br>0.00 (0.00 to 4.57) | 1.99 (1.73)<br>3.00 (0.00 to 4.31) | <0.001 |
| $A_{apexpost}$ ($mm^2$) | 4.32 (0.26)<br>4.31 (3.58 to 5.00) | 3.51 (0.52)<br>3.71 (2.00 to 5.00) | <0.001 |
| $A_{mctant}$ ($mm^2$) | 4.15 (0.37)<br>4.07 (3.00 to 5.01) | 3.50 (0.52)<br>3.63 (2.00 to 5.00) | <0.001 |
| $A_{mctpost}$ ($mm^2$) | 4.31 (0.26)<br>4.32 (3.57 to 5.01) | 3.50 (0.51)<br>3.65 (2.00 to 5.00) | <0.001 |
| $D_{apexant}$ (mm) | 0.000 (0.001)<br>0.000 (0.000 to 0.007) | 0.011 (0.017)<br>0.003 (0.000 to 0.070) | <0.001 |
| $D_{apexpost}$ (mm) | 0.073 (0.053)<br>0.067 (0.024 to 0.650) | 0.186 (0.095)<br>0.175 (0.011 to 0.594) | <0.001 |
| $D_{mctant}$ (mm) | 0.879 (0.253)<br>0.844 (0.438 to 2.171) | 0.907 (0.279)<br>0.973 (0.160 to 2.051) | 0.314 |
| $D_{mctpost}$ (mm) | 0.806 (0.235)<br>0.794 (0.375 to 2.059) | 0.861 (0.266)<br>0.904 (0.104 to 2.000) | 0.035 |

Abbreviations: SD, standard deviation; $A_{ant}$, anterior corneal surface area; $A_{post}$, posterior corneal surface area; $A_{tot}$, total corneal surface area; $A_{apexant}$ and $A_{apexpost}$, area of the cornea within the sagittal plane passing through the Z axis and the highest point (apex) of the anterior or posterior corneal surface; $A_{mctant}$ and $A_{mctpost}$, area of the cornea within the sagittal plane passing through the Z axis and the minimum thickness point of the anterior and posterior corneal surfaces; $D_{apexant}$ and $D_{apexpost}$, average distance from the Z axis to the highest point (apex) of the anterior and posterior corneal surfaces; $D_{mctant}$ and $D_{mctpost}$, average distance in the XY plane from the Z axis to the minimum thickness points (maximum curvature) of the anterior and posterior corneal surfaces.

https://doi.org/10.1371/journal.pone.0184569.t002

**Table 3. Summary of the outcomes obtained in control group and keratoconus subgroups according to the stage of severity of the disease.**

| Mean (SD) Median (Range) | Control (C) | Ktc grade I (KC1) | Ktc grade II (KC2) | Ktc grade III (KC3) | Ktc grade IV (KC4) | p-valor (test) |
|---|---|---|---|---|---|---|
| $A_{ant}$ ($mm^2$) | 43.08 (0.14)<br>43.08 (42.73 to 43.39) | 42.93 (0.33)<br>43.00 (42.00 to 43.58) | 43.29 (0.42)<br>43.00 (43.00 to 45.00) | 43.97 (0.21)<br>44.00 (43.52 to 44.35) | 44.22 (0.93)<br>44.00 (43.00 to 47.00) | <0.001 |
| $A_{post}$ ($mm^2$) | 44.24 (0.28)<br>44.24 (43.49 to 44.90) | 44.07 (0.42)<br>44.00 (43.00 to 45.07) | 44.84 (0.59)<br>45.00 (44.00 to 47.00) | 45.60 (0.49)<br>45.78 (44.87 to 46.00) | 46.37 (1.42)<br>46.00 (44.39 to 51.00) | <0.001 |
| $A_{tot}$ ($mm^2$) | 103.92 (1.20)<br>103.88 (100.69 to 106.15) | 103.10 (1.33)<br>103.00 (100.00 to 107.00) | 104.10 (1.43)<br>104.00 (99.96 to 109.00) | 104.55 (1.97)<br>105.48 (101.00 to 106.00) | 107.34 (2.93)<br>106.74 (103.00 to 114.00) | <0.001 |
| $A_{apexant}$ ($mm^2$) | 0.24 (1.01)<br>0.00 (0.00 to 4.57) | 1.55 (1.78)<br>0.00 (0.00 to 4.31) | 3.10 (0.98)<br>3.00 (0.00 to 4.00) | 2.56 (1.01)<br>3.00 (0.00 to 3.00) | 3.21 (0.83)<br>3.00 (0.00 to 4.00) | <0.001 |
| $A_{apexpost}$ ($mm^2$) | 4.32 (0.26)<br>4.31 (3.58 to 5.00) | 3.55 (0.52)<br>3.95 (2.00 to 5.00) | 3.47 (0.53)<br>3.56 (2.00 to 4.48) | 3.04 (0.49)<br>3.00 (2.00 to 3.70) | 3.37 (0.50)<br>3.00 (3.00 to 4.27) | <0.001 |
| $A_{mctant}$ ($mm^2$) | 4.15 (0.37)<br>4.07 (3.00 to 5.01) | 3.54 (0.52)<br>3.87 (2.00 to 5.00) | 3.46 (0.53)<br>3.53 (2.00 to 4.48) | 3.04 (0.49)<br>3.00 (2.00 to 3.69) | 3.33 (0.48)<br>3.00 (3.00 to 4.27) | <0.001 |
| $A_{mctpost}$ ($mm^2$) | 4.31 (0.26)<br>4.32 (3.57 to 5.01) | 3.54 (0.52)<br>3.87 (2.00 to 5.00) | 3.50 (0.49)<br>3.63 (3.00 to 4.48) | 3.15 (0.30)<br>3.00 (2.99 to 3.69) | 3.33 (0.48)<br>3.00 (3.00 to 4.27) | <0.001 |
| $D_{apexant}$ (mm) | 0.000 (0.001)<br>0.000 (0.000 to 0.007) | 0.006 (0.012)<br>0.000 (0.000 to 0.070) | 0.022 (0.021)<br>0.012 (0.000 to 0.069) | 0.022 (0.023)<br>0.014 (0.000 to 0.066) | 0.024 (0.019)<br>0.019 (0.000 to 0.066) | <0.001 |
| $D_{apexpost}$ (mm) | 0.073 (0.053)<br>0.067 (0.024 to 0.650) | 0.170 (0.088)<br>0.160 (0.011 to 0.594) | 0.211 (0.101)<br>0.197 (0.026 to 0.453) | 0.217 (0.096)<br>0.221 (0.054 to 0.368) | 0.266 (0.097)<br>0.290 (0.052 to 0.412) | <0.001 |
| $D_{mctant}$ (mm) | 0.879 (0.253)<br>0.844 (0.438 to 2.171) | 0.934 (0.266)<br>1.000 (0.336 to 2.051) | 0.893 (0.317)<br>0.856 (0.307 to 1.828) | 0.680 (0.250)<br>0.697 (0.233 to 1.000) | 0.766 (0.247)<br>0.856 (0.160 to 1.000) | 0.003 |
| $D_{mctpost}$ (mm) | 0.806 (0.235)<br>0.794 (0.375 to 2.059) | 0.889 (0.249)<br>0.953 (0.319 to 2.000) | 0.840 (0.306)<br>0.791 (0.267 to 1.725) | 0.633 (0.256)<br>0.631 (0.197 to 1.000) | 0.728 (0.252)<br>0.809 (0.104 to 1.000) | <0.001 |

Abbreviations: SD, standard deviation; $A_{ant}$, anterior corneal surface area; $A_{post}$, posterior corneal surface area; $A_{tot}$, total corneal surface area; $A_{apexant}$ and $A_{apexpost}$, area of the cornea within the sagittal plane passing through the Z axis and the highest point (apex) of the anterior or posterior corneal surface; $A_{mctant}$ and $A_{mctpost}$, area of the cornea within the sagittal plane passing through the Z axis and the minimum thickness point of the anterior and posterior corneal surfaces; $D_{apexant}$ and $D_{apexpost}$, average distance from the Z axis to the highest point (apex) of the anterior and posterior corneal surfaces; $D_{mctant}$ and $D_{mctpost}$, average distance in the XY plane from the Z axis to the minimum thickness points (maximum curvature) of the anterior and posterior corneal surfaces

https://doi.org/10.1371/journal.pone.0184569.t003

the keratoconus subgroups according to the stage of severity of the disease. As shown, strong correlations among $A_{ant}$ and $A_{post}$ were found in both control and keratoconus groups. However, when the results are analyzed according to keratoconus severity, a stronger correlation

**Table 4. Summary of the correlations obtained between the geometric parameters of the anterior and posterior corneal surfaces in the control group and keratoconus subgroups according to the stage of severity of the disease.**

| Correlation coefficient (p-value) | Control (C) | Keratoconus (KC) | Ktc grade I (KC1) | Ktc grade II (KC2) | Ktc grade III (KC3) | Ktc grade IV (KC4) |
|---|---|---|---|---|---|---|
| $A_{ant}$-$A_{post}$ | 0.825 (p<0.001) | 0.836 (p<0.001) | 0.493 (p<0.001) | 0.585 (p<0.001) | 0.436 (p = 0.241) | 0.943 (p<0.001) |
| $A_{apexant}$-$A_{apexpost}$ | 0.051 (p = 0.544) | 0.076 (p = 0.176) | 0.125 (p = 0.058) | 0.153 (p = 0.247) | -0.217 (p = 0.576) | 0.567 (p = 0.004) |
| $A_{mctant}$-$A_{mctpost}$ | 0.677 (p<0.001) | 0.983 (p<0.001) | 0.999 (p<0.001) | 0.938 (p<0.001) | 0.742 (p = 0.022) | 0.999 (p<0.001) |
| $D_{apexant}$—$D_{apexpost}$ | 0.031 (p = 0.712) | 0.396 (p<0.001) | 0.328 (p<0.001) | 0.320 (p = 0.014) | -0.073 (p = 0.853) | 0.478 (p = 0.018) |
| $D_{mctant}$—$D_{mctpost}$ | 0.982 (p<0.001) | 0.954 (p<0.001) | 0.931 (p<0.001) | 0.994 (p<0.001) | 0.993 (p<0.001) | 0.987 (p<0.001) |

Abbreviations: $A_{ant}$, anterior corneal surface area; $A_{post}$, posterior corneal surface area; $A_{apexant}$ and $A_{apexpost}$, area of the cornea within the sagittal plane passing through the Z axis and the highest point (apex) of the anterior or posterior corneal surface; $A_{mctant}$ and $A_{mctpost}$, area of the cornea within the sagittal plane passing through the Z axis and the minimum thickness point of the anterior and posterior corneal surfaces; $D_{apexant}$ and $D_{apexpost}$, average distance from the Z axis to the highest point (apex) of the anterior and posterior corneal surfaces; $D_{mctant}$ and $D_{mctpost}$, average distance in the XY plane from the Z axis to the minimum thickness points (maximum curvature) of the anterior and posterior corneal surfaces

https://doi.org/10.1371/journal.pone.0184569.t004

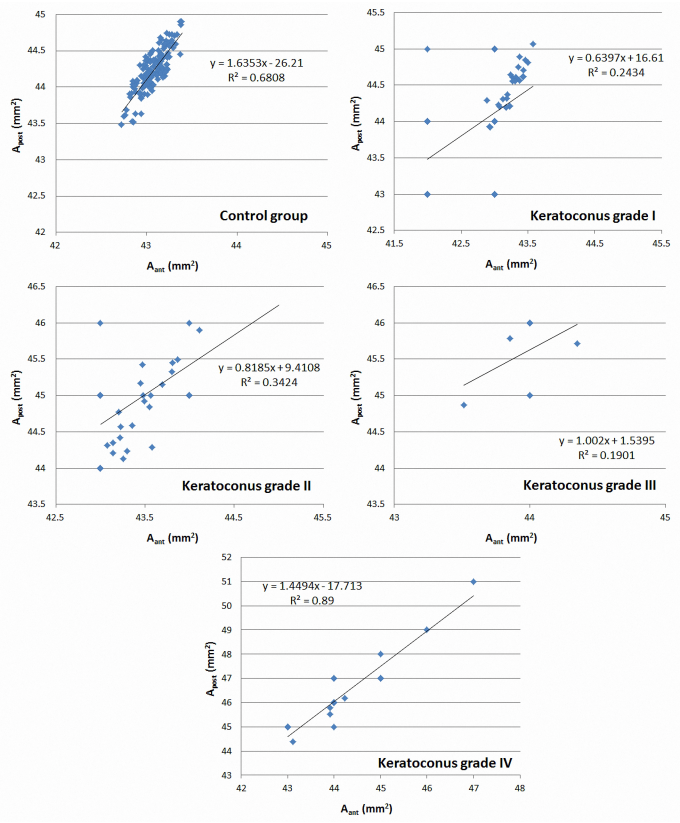


**Fig 5. Scatterplots showing the relationship between the areas of the anterior corneal surface ($A_{ant}$) and posterior corneal surface area ($A_{post}$).** The adjusting line to the data obtained by means of the least-squares fit is shown.

https://doi.org/10.1371/journal.pone.0184569.g005

between $A_{ant}$ and $A_{post}$ was observed in eyes with severe keratoconus compared to the rest (Fig 5). No significant correlations were found between $A_{apexant}$ and $A_{apexpost}$ in control group and keratoconus grade I, II and III subgroups. However, the correlation between these two parameters was strong in keratoconus grade IV subgroup. Similarly, the correlation between $D_{apexant}$ and $D_{apexpost}$ became stronger and statistically significant in keratoconus grade IV compared to the rest. Regarding the correlation between $A_{mctant}$ and $A_{mctpost}$, it was good and statistically significant in all keratoconus subgroups, but somewhat weaker in control group. A very strong correlation among $D_{mctant}$ and $D_{mctpost}$ was found in all groups and subgroups.

## Predictive model for subclinical keratoconus detection

The logistic regression analysis revealed that the detection of keratoconus grade I was related to the variables $A_{post}$, $A_{tot}$, $A_{apexant}$, $A_{mctant}$, $A_{mctpost}$, $D_{apexpost}$, $D_{mctant}$ and $D_{mctpost}$ ($p>0.05$, Chi-Square and Hosmer-Lemeshow). The coefficient of determination $R^2$ Cox and Snell (general) was 0.681, while the $R^2$ Nagelkerke (corrected) was 0.926. Table 5 shows the model coefficients (B), the statistical significance, the exponential of B (ExpB, odds ratio) and confidence interval 95% of ExpB for each variable in the model. Specifically, the model revealed that the probability of having keratoconus grade I is 79.91 times higher for each $mm^2$ increase of $A_{tot}$, 1.77 times higher for each $mm^2$ increase of $A_{apexant}$, $5.99 \times 10^{31}$ times higher for each $mm^2$ increase of $A_{mctant}$, $1.58 \times 10^{9}$ times higher for each mm increase of $D_{apexpost}$, and $5.511 \times 10^{7}$ times higher for each mm increase of $D_{mctpost}$. The overall percentage of cases correctly

**Table 5. Summary of model defined for detection of early keratoconus.**

| | B | Sig | ExpB | CI 95% for ExpB |
|---|---|---|---|---|
| $A_{post}$ ($mm^2$) | -8.99 | 0.001 | $1.250x10^{-4}$ | $6.200x10^{-7}$ to 0.025 |
| $A_{tot}$ ($mm^2$) | 4.38 | <0.001 | 79.911 | 8.518 to 749.706 |
| $A_{apexant}$ ($mm^2$) | 0.57 | 0.009 | 1.768 | 1.155 to 2.706 |
| $A_{mctant}$ ($mm^2$) | 73.17 | 0.256 | $5.989x10^{31}$ | $9.086x10^{-24}$ to $3.947x10^{86}$ |
| $A_{mctpost}$ ($mm^2$) | -96.94 | 0.135 | $7.947x10^{-43}$ | $4.420x10^{-98}$ to $1.429x10^{13}$ |
| $D_{apexpost}$ (mm) | 21.18 | 0.001 | $1.576x10^{9}$ | $7.153x10^{3}$ to $3.473x10^{14}$ |
| $D_{mctant}$ (mm) | -17.33 | 0.052 | $2.982x10^{-8}$ | $7.859x10^{-16}$ to 1.132 |
| $D_{mctpost}$ (mm) | 17.83 | 0.058 | $5.511x10^{7}$ | 0.532 to $5.705x10^{15}$ |
| **Constant of the model** | 40.06 | 0.358 | $2.486x10^{17}$ | |

Abbreviations: $A_{post}$, posterior corneal surface area; $A_{tot}$, total corneal surface area; $A_{apexant}$, area of the cornea within the sagittal plane passing through the Z axis and the highest point (apex) of the anterior corneal surface; $A_{mctant}$ and $A_{mctpost}$, area of the cornea within the sagittal plane passing through the Z axis and the minimum thickness point of the anterior and posterior corneal surfaces; $D_{apexpost}$, average distance from the Z axis to the highest point (apex) of the posterior corneal surface; $D_{mctant}$ and $D_{mctpost}$, average distance in the XY plane from the Z axis to the minimum thickness points (maximum curvature) of the anterior and posterior corneal surfaces

https://doi.org/10.1371/journal.pone.0184569.t005

classified by our model was 97.30% (97.2% control group, 97.4% keratoconus grade I subgroup), whereas the percentage of cases correctly identified by the classifier of the topography system was 91.94% (97.9% control group, 88.2%).

## Discussion

The development of more sensitive algorithms for the detection of most incipient cases of keratoconus is currently of great interest as there are several therapeutic options that would allow halting the progression of the disease. In this line, we have tried to define a new predictive model for the detection of incipient keratoconus but based on a previously developed morphogeometric modeling of the cornea [16]. There is already a great variety of indices and diagnostic systems defined for the detection of keratoconus [2], but most of them are based on the analysis of curvature changes or asymmetries of both posterior corneal surfaces [4, 5, 8, 14, 15]. Likewise, corneal elevation [6, 7], corneal aberrometric [11], and pachymetric algorithms [10] have been also defined for the detection of keratoconus as well as the indirect measurement of some biomechanical parameters [9, 12]. However, few approaches have been developed for keratoconus detection considering the cornea as a solid with a specific volume [14], including an evaluation of the relationship between different sections of this solid [16]. This type of analysis may contribute to a better differentiation between healthy and pathological corneas and supposes a new concept in the characterization of the corneal structure in keratoconus. In our approach, we have defined and analyzed the following variables: the areas of the anterior and posterior corneal surfaces of the solid model generated ($A_{ant}$, $A_{post}$), the total corneal surface area ($A_{tot}$), the areas of the cornea within the sagittal plane passing through the Z axis and the highest point of both corneal surfaces ($A_{apexant}$, $A_{apexpost}$), the areas of the cornea within the sagittal plane passing through the Z axis and the minimum thickness point of both corneal surfaces ($A_{mctant}$, $A_{mctpost}$) corneal surfaces, the average distance from the Z axis to the highest point of the anterior and posterior corneal surfaces ($D_{apexant}$, $D_{apexpost}$), and the average distance in the XY plane from the Z axis to the minimum thickness points of the anterior and posterior corneal surfaces ($D_{mctant}$, $D_{mctpost}$). We demonstrated in a previous study evaluating a significantly smaller sample of eyes that some of these parameters provided a good diagnostic ability for the detection of keratoconus ($A_{ant}$, $A_{post}$, $A_{apexant}$, and $A_{apexpost}$) [16]. The

current study was aimed at studying the distribution of the new geometric variables defined in the healthy and keratoconus population and to define a new model of detection of early keratoconus based on the combination of these variables.

In our sample of 143 healthy eyes and 321 eyes with keratoconus, we found significant differences among groups in $A_{post}$, $A_{apexant}$, $A_{apexpost}$, $A_{mctant}$, $A_{mctpost}$, $D_{apexant}$, $D_{apexpost}$, and $D_{mctpost}$. This is consistent with the results found in our previous preliminary study conducted on 41 keratoconus eyes [16]. These results confirms that changes occurring in posterior corneal surface in keratoconus lead to an increase of the area corresponding to such surface ($A_{post}$). This is mainly due to the localized steepening that occur in this surface in the area of the cone, with no significant flattening in the periphery [4, 5, 14, 15]. This generates that the area occupied by this surface would be significantly higher. In contrast, this does not happen with $A_{ant}$, as steepening areas in anterior corneal surface in keratoconus are not so relevant in incipient stages but are very marked in moderate and advanced cases, which introduces a significant variability in the analysis of this parameter [2, 4, 5, 14, 15].

The analysis of $A_{apexant}$ data revealed that a significantly lower value of this area was present in healthy eyes compared to keratoconus. However, the trend was the opposite for $A_{apexpost}$, with lower values in keratoconus group. This is consistent with changes in the position of the apex of the anterior corneal surface in keratoconus eyes. It should be considered that the point of maximum elevation in keratoconus is displaced in most of cases inferiorly close to or coincident with the point of minimum thickness, even in incipient cases [2, 19–21]. Abu Ameerh et al [20] found in a sample of 210 patients with keratoconus that the vertical apex location correlated well with severity levels while the horizontal location seemed to have no effect. In our sample, $A_{apexant}$ increased as the severity of keratoconus was higher, confirming that the displacement of the apex of the anterior corneal surface is an effect related to the progression of the disease. However, this trend was not observed for $A_{apexpost}$, with higher values in the control group compared to the keratoconus group and subgroups. This suggests that there is some level of displacement of the posterior corneal apex compared to the sagittal plane passing through the Z axis in the posterior corneal surface in the healthy eye. Therefore, a change in this displacement would a sign related to the corneal ectatic process. This is consistent with studies reporting an asymmetric distribution of corneal pachymetry derived from the relationship among the elevation of both corneal surfaces in normal healthy corneas [22]. Jonuscheit et al [22] demonstrated that the nasal-temporal asymmetry of 113 healthy eyes became greater with increasing distance from the corneal center, with a mean difference of 59 ± 22 μm at 4 mm from the apex.

Regarding $A_{mctant}$ and $A_{mctpost}$, we found that both areas were significantly lower in keratoconus corneas compared to control group, with no clear differences among keratoconus severity subgroups. This suggests that although the position of minimal thickness is altered in keratoconus, this alteration is not coincident with that observed in the corneal apex or the point of maximum elevation. Indeed, Auffarth et al [21] demonstrated several years ago that there was a significant distance in keratoconus corneas between the apex and the thinnest point. Specifically, they found a mean value for this distance of 0.917 ± 0.729 mm [21]. Therefore, we cannot state that the point of minimum thickness and the corneal apex are coincident in all keratoconus cases. Indeed, significant differences among keratoconus and control groups were found in our sample for $D_{apexant}$ and $D_{apexpost}$, which is the distance from the Z axis to the point of maximum height (apex) of the anterior and posterior corneal surfaces, but not for $D_{mctant}$, which is the distance from the Z axis to the point of minimum corneal thickness of the anterior corneal surface.

Significant correlations were found among the parameters defined for anterior and posterior corneal surfaces, except for the correlations between $A_{apexant}$ and $A_{apexpost}$, and also

between $D_{apexant}$ and $D_{apexpost}$. This confirms that changes occurring in the points corresponding to the minimum corneal thickness in the anterior and posterior corneal surfaces as well as the area of each surface are correlated. This is consistent with the results of previous studies evaluating the correlation of standard geometric parameters of anterior and posterior corneal surfaces in keratoconus [4, 5, 14, 15]. Our research group have found in previous studies correlations between anterior and posterior corneal surfaces in terms of curvature, asphericity and astigmatism [4, 14, 15]. Curvature and asphericity changes of both corneal surfaces in keratoconus are related to the area of each surface and for this reason we also obtained a correlation between the areas calculated with our geometric approach for both surfaces. Furthermore, we found in our series an increased strength of the correlation between $A_{ant}$ and $A_{post}$ as the severity of the keratoconus increases, suggesting that an increasing area of steepening surrounded by an increasing area of corneal flattening is present as the severity of the disease is also increased. This is consistent with the definition of the course of the disease [1, 2] and therefore confirms that our approach is also reflecting the changes occurring in keratoconus but from another perspective. As a new finding, we have confirmed that changes in the apex of both corneal surfaces are not correlated in keratoconus, except for those eyes with an advanced stage of the disease. To our knowledge, this is the first study reporting this outcome.

Finally, we have obtained by logistic regression a new model of detection of early keratoconus (only grade I) considering the new parameters defined according to our new geometric approach. It should be considered that moderate and advanced keratoconus can be easily detected by means of conventional topographic analyses and the real challenge is to detect with accuracy those cases of keratoconus in an incipient stage. We found that considering $A_{post}$, $A_{tot}$, $A_{apexant}$, $A_{mctant}$, $A_{mctpost}$, $D_{apexpost}$, $D_{mctant}$ and $D_{mctpost}$, a detection of keratoconus grade I could be done with sensitivity of 97.4% and specificity of 97.2%. However, the percentage of cases correctly identified by the classifier of the topography system was 91.94%. The levels of sensitivity and specificity found are equivalent and even better than those reported by other different models of keratoconus detection based on standard topographic analysis [18, 19, 23–27]. The cone location and magnitude index (CLMI) combining different topographic parameters has shown to provide a keratoconus detection accuracy of 92% [23]. The SCORE Analyzer which integrates the data obtained with a scanning-slit topography system allows the detection of keratoconus with sensitivity and specificity of 92% and 96%, respectively [27]. The Sirius topography system includes a keratoconus detection analysis that has been reported to provide true predictions in around 93% of cases or more [18]. In our sample, the percentage of true predictions was close to 92%, a value below the true predictions obtained with our model. Future studies should confirm if our model of detection can be also applied with accuracy for the detection of subclinical keratoconus or if some adjustments are necessary to optimize the levels of sensitivity and specificity of the model.

In conclusion, a new geometric approach based on the analysis of the cornea as a solid with a specific volume, including an evaluation of the relationship between different sections of this solid, is a useful tool for the detection of keratoconus. The use of the combination of a variety of parameters based on this geometric approach is highly sensitive and specific for an accurate detection of incipient keratoconus cases.

## Supporting information

**S1 Table. Demographics of the study population (control and keratoconus).**
(XLSX)

**S2 Table. Summary of the outcomes obtained in control group and keratoconus subgroups according to the stage of severity of the disease (extended information).**
(DOCX)

## Author Contributions

**Conceptualization:** Francisco Cavas-Martínez.

**Data curation:** Laurent Bataille.

**Formal analysis:** Laurent Bataille, Francisco J. F. Cañavate.

**Funding acquisition:** Jorge L. Alió.

**Investigation:** Francisco Cavas-Martínez.

**Methodology:** Francisco Cavas-Martínez, Daniel G. Fernández-Pacheco.

**Project administration:** Jorge L. Alió.

**Resources:** Laurent Bataille.

**Software:** Daniel G. Fernández-Pacheco, Francisco J. F. Cañavate.

**Supervision:** Jorge L. Alió.

**Validation:** Francisco Cavas-Martínez.

**Visualization:** Francisco J. F. Cañavate.

**Writing – original draft:** Francisco Cavas-Martínez, Daniel G. Fernández-Pacheco.

**Writing – review & editing:** Francisco Cavas-Martínez, Daniel G. Fernández-Pacheco, Jorge L. Alió.

## References

1. Alio JL, Pinero DP, Aleson A, Teus MA, Barraquer RI, Murta J, et al. Keratoconus-integrated characterization considering anterior corneal aberrations, internal astigmatism, and corneal biomechanics. Journal of cataract and refractive surgery. 2011; 37(3):552–68. Epub 2011/02/22. https://doi.org/10.1016/j.jcrs.2010.10.046 PMID: 21333878.
2. Pinero DP, Nieto JC, Lopez-Miguel A. Characterization of corneal structure in keratoconus. Journal of cataract and refractive surgery. 2012; 38(12):2167–83. Epub 2012/12/01. https://doi.org/10.1016/j.jcrs.2012.10.022 PMID: 23195256.
3. Rabinowitz YS. Keratoconus. Survey of ophthalmology. 1998; 42(4):297–319. Epub 1998/03/11. PMID: 9493273.
4. Montalbán R, Alio JL, Javaloy J, Piñero DP. Comparative analysis of the relationship between anterior and posterior corneal shape analyzed by Scheimpflug photography in normal and keratoconus eyes. Graefe's Archive for Clinical and Experimental Ophthalmology. 2013; 251(6):1547–55. https://doi.org/10.1007/s00417-013-2261-3 PMID: 23334367
5. Tomidokoro A, Oshika T, Amano S, Higaki S, Maeda N, Miyata K. Changes in anterior and posterior corneal curvatures in keratoconus. Ophthalmology. 2000; 107(7):1328–32. Epub 2000/07/13. PMID: 10889107.
6. de Sanctis U, Loiacono C, Richiardi L, Turco D, Mutani B, Grignolo FM. Sensitivity and specificity of posterior corneal elevation measured by Pentacam in discriminating keratoconus/subclinical keratoconus. Ophthalmology. 2008; 115(9):1534–9. Epub 2008/04/15. https://doi.org/10.1016/j.ophtha.2008.02.020 PMID: 18405974.
7. Jafarinasab MR, Shirzadeh E, Feizi S, Karimian F, Akaberi A, Hasanpour H. Sensitivity and specificity of posterior and anterior corneal elevation measured by orbscan in diagnosis of clinical and subclinical keratoconus. Journal of ophthalmic & vision research. 2015; 10(1):10–5. Epub 2015/05/26. https://doi.org/10.4103/2008-322x.156085 PMID: 26005546; PubMed Central PMCID: PMCPmc4424711.

8. Ramos-Lopez D, Martinez-Finkelshtein A, Castro-Luna GM, Burguera-Gimenez N, Vega-Estrada A, Pinero D, et al. Screening subclinical keratoconus with placido-based corneal indices. Optometry and vision science: official publication of the American Academy of Optometry. 2013; 90(4):335–43. Epub 2013/02/05. https://doi.org/10.1097/OPX.0b013e3182843f2a PMID: 23376898.
9. Kozobolis V, Sideroudi H, Giarmoukakis A, Gkika M, Labiris G. Corneal biomechanical properties and anterior segment parameters in forme fruste keratoconus. European journal of ophthalmology. 2012; 22 (6):920–30. Epub 2012/08/07. https://doi.org/10.5301/ejo.5000184 PMID: 22865401.
10. Prakash G, Agarwal A, Mazhari AI, Kumar G, Desai P, Kumar DA, et al. A new, pachymetry-based approach for diagnostic cutoffs for normal, suspect and keratoconic cornea. Eye (London, England). 2012; 26(5):650–7. Epub 2012/01/28. https://doi.org/10.1038/eye.2011.365 PMID: 22281864; PubMed Central PMCID: PMCPmc3351046.
11. Gordon-Shaag A, Millodot M, Ifrah R, Shneor E. Aberrations and topography in normal, keratoconus-suspect, and keratoconic eyes. Optometry and vision science: official publication of the American Academy of Optometry. 2012; 89(4):411–8. Epub 2012/02/09. https://doi.org/10.1097/OPX.0b013e318249d727 PMID: 22311193.
12. Touboul D, Benard A, Mahmoud AM, Gallois A, Colin J, Roberts CJ. Early biomechanical keratoconus pattern measured with an ocular response analyzer: curve analysis. Journal of cataract and refractive surgery. 2011; 37(12):2144–50. Epub 2011/10/08. https://doi.org/10.1016/j.jcrs.2011.06.029 PMID: 21978610.
13. Ucakhan OO, Cetinkor V, Ozkan M, Kanpolat A. Evaluation of Scheimpflug imaging parameters in subclinical keratoconus, keratoconus, and normal eyes. Journal of cataract and refractive surgery. 2011; 37(6):1116–24. Epub 2011/05/21. https://doi.org/10.1016/j.jcrs.2010.12.049 PMID: 21596255.
14. Pinero DP, Alio JL, Aleson A, Escaf Vergara M, Miranda M. Corneal volume, pachymetry, and correlation of anterior and posterior corneal shape in subclinical and different stages of clinical keratoconus. Journal of cataract and refractive surgery. 2010; 36(5):814–25. Epub 2010/05/12. https://doi.org/10.1016/j.jcrs.2009.11.012 PMID: 20457375.
15. Montalban R, Alio JL, Javaloy J, Pinero DP. Correlation of anterior and posterior corneal shape in keratoconus. Cornea. 2013; 32(7):916–21. Epub 2013/05/15. https://doi.org/10.1097/ICO.0b013e3182904950 PMID: 23665644.
16. Cavas-Martínez F, Fernández-Pacheco DG, De la Cruz-Sánchez E, Nieto Martínez J, Fernández Cañavate FJ, Vega-Estrada A, et al. Geometrical Custom Modeling of Human Cornea In Vivo and Its Use for the Diagnosis of Corneal Ectasia. PLOS ONE. 2014; 9(10):e110249. https://doi.org/10.1371/journal.pone.0110249 PMID: 25329896
17. Montalban R, Alio JL, Javaloy J, Pinero DP. Intrasubject repeatability in keratoconus-eye measurements obtained with a new Scheimpflug photography-based system. Journal of cataract and refractive surgery. 2013; 39(2):211–8. Epub 2012/12/12. https://doi.org/10.1016/j.jcrs.2012.10.033 PMID: 23218818.
18. Arbelaez MC, Versaci F, Vestri G, Barboni P, Savini G. Use of a support vector machine for keratoconus and subclinical keratoconus detection by topographic and tomographic data. Ophthalmology. 2012; 119 (11):2231–8. Epub 2012/08/16. https://doi.org/10.1016/j.ophtha.2012.06.005 PMID: 22892148.
19. Wahba SS, Roshdy MM. Rotating Scheimpflug Imaging Indices in Different Grades of Keratoconus. Journal of ophthalmology. 2016; 2016:6392472. https://doi.org/10.1155/2016/6392472 PMID: 27579178.
20. Abu Ameerh MA, Bussieres N, Hamad GI, Al Bdour MD. Topographic characteristics of keratoconus among a sample of Jordanian patients. International journal of ophthalmology. 2014; 7(4):714–9. Epub 2014/08/28. https://doi.org/10.3980/j.issn.2222-3959.2014.04.24 PMID: 25161949; PubMed Central PMCID: PMCPmc4137213.
21. Auffarth GU, Wang L, Volcker HE. Keratoconus evaluation using the Orbscan Topography System. Journal of cataract and refractive surgery. 2000; 26(2):222–8. Epub 2000/02/23. PMID: 10683789.
22. Jonuscheit S, Doughty MJ, Martin R, Rio-Cristobal A, Cruikshank V, Lang S. Peripheral nasal-temporal corneal asymmetry in relation to corneal thickness: a Scheimpflug imaging study. Ophthalmic & physiological optics: the journal of the British College of Ophthalmic Opticians (Optometrists). 2015; 35(1):45–51. Epub 2014/12/24. https://doi.org/10.1111/opo.12179 PMID: 25532545.
23. Kocamis SI, Cakmak HB, Cagil N, Toklu Y. Investigation of the Efficacy of the Cone Location and Magnitude Index in the Diagnosis of Keratoconus. Seminars in ophthalmology. 2016; 31(3):203–9. Epub 2014/05/21. https://doi.org/10.3109/08820538.2014.914234 PMID: 24840348.
24. Steinberg J, Aubke-Schultz S, Frings A, Hulle J, Druchkiv V, Richard G, et al. Correlation of the KISA% index and Scheimpflug tomography in 'normal', 'subclinical', 'keratoconus-suspect' and 'clinically manifest' keratoconus eyes. Acta ophthalmologica. 2015; 93(3):e199–207. Epub 2015/04/16. https://doi.org/10.1111/aos.12590 PMID: 25873278.

25. Ruisenor Vazquez PR, Galletti JD, Minguez N, Delrivo M, Fuentes Bonthoux F, Pfortner T, et al. Pentacam Scheimpflug tomography findings in topographically normal patients and subclinical keratoconus cases. American journal of ophthalmology. 2014; 158(1):32–40.e2. Epub 2014/04/09. https://doi.org/10.1016/j.ajo.2014.03.018 PMID: 24709808.

26. Mahmoud AM, Nunez MX, Blanco C, Koch DD, Wang L, Weikert MP, et al. Expanding the cone location and magnitude index to include corneal thickness and posterior surface information for the detection of keratoconus. American journal of ophthalmology. 2013; 156(6):1102–11. Epub 2013/10/01. https://doi.org/10.1016/j.ajo.2013.07.018 PMID: 24075426.

27. Saad A, Gatinel D. Validation of a New Scoring System for the Detection of Early Forme of Keratoconus. International Journal of Keratoconus and Ectatic Corneal Diseases. 2012; 1(2):100–8. https://doi.org/10.5005/jp-journals-10025-1019